Hyperfine Interaction (2018) 239:46
https://doi.org/10.1007/s10751-018-1513-3

Oxidation and passivating effect in tin(II) fluoride and chloride fluoride solid solutions: a ^{119}Sn Mössbauer study

Georges Dénès[1] · Abdualhafed Muntasar[1] · M. Cecilia Madamba[1] · Hocine Merazig[2]

Published online: 25 October 2018

Abstract
Divalent tin fluorides and chloride fluorides appear to be stable relative to oxidation to tetravalent tin at ambient temperature. X-ray diffraction shows only the line of the tin(II) compound, however the ^{119}Sn Mössbauer spectrum of all tin(II) polycrystalline samples has a small broad peak at ca. 0 mm/s. This is the case of polycrystalline $\alpha-SnF_2$, while the spectrum of a large single crystal polished sufficiently thin shows only the tin(II) doublet, with no SnO_2 peak at 0 mm/s. This shows that there is surface oxidation of each solid particle, to give a thin amorphous layer of SnO_2 stannic oxide. However, the Mössbauer peak of SnO_2 does not grow with prolonged exposure to air at ambient temperature, therefore it must be assumed that the layer of SnO_2 has a passivating effect, however oxidation increases at higher temperatures. We have investigated in this work the passivating effect of a layer of SnO_2 in two types of solid solutions: (i) in the fluorite type $M_{1-x}Sn_xF_2$, where the amount of tin at low x values is not sufficient to provide full coverage of the surface of the particles, and (ii) in the PbClF type doubly disordered solid solution, $Ba_{1-x}Sn_xCl_{1+y}F_{1-y}$. It was found that passivation works well in the $M_{1-x}Sn_xF_2$ solid solution, however most of the time, it does not work so well for $Ba_{1-x}Sn_xCl_{1+y}F_{1-y}$ where it is strongly dependent on the method of preparation and the bonding strength, as shown by the variation versus the tin(II) recoil-free fraction.

Keywords Mössbauer spectroscopy · Tin(II) fluorides and chloride fluorides · Surface oxidation · Passivation · Solid solutions · Bonding type

This article is part of the Topical Collection on *Proceedings of the 4th Mediterranean Conference on the Applications of the Mössbauer Effect (MECAME 2018), Zadar, Croatia, 27-31 May 2018*
Edited by Mira Ristic and Stjepko Krehula

✉ Georges Dénès
georges.denes@concordia.ca; madenes@videotron.ca

[1] Laboratory of Solid State Chemistry and Mössbauer Spectroscopy, Department of Chemistry and Biochemistry, Concordia University, Montréal, Québec, Canada

[2] Unité de Recherche de Chimie de l'Environnement et Moléculaire Structurale CHEMS, Université des Frères Mentouri de Constantine, Constantine, Algeria

1 Introduction

Tin is a main group element that belongs to group 14 of the periodic table. Its electronic structure is [Kr] $4d^{10}\ 5s^2\ 5p^2$. It has four valence electrons, and therefore, its full oxidation state (= oxidation number) is +4. However, going down each group, from group 13 to 18, the energy difference between the ns and the np subshells increases sufficiently to make it possible to lose only the np electrons to form cations or to use only them to form covalent bonds, while the two electrons of the ns subshell remain in the form of a *non-bonded electron pair* (*lone pair*), thereby creating a sub-oxidation state. In the case of tin, the +2 oxidation number is sufficiently stable to make it possible to isolate divalent tin compounds that appear to be stable relative to oxidation at ambient temperature, even in air, for indefinite periods of time. In contrast, germanium, above tin in group 14, is very rarely found in the +2 suboxidation number, and such compounds are very highly unstable in air, while for lead below tin in group 14, the +2 oxidation number is very stable, even much more stable than the +4 full oxidation number, with lead(IV) compounds being strong oxidizers. This trend is due to the contraction of atomic orbitals for heavy atoms when the electrons approach relativistic speeds, as explained by Dirac's relativistic quantum mechanics [1]. Therefore tin stands between germanium with the divalent state being very unstable and lead with the divalent state being more stable than the tetravalent state. The question is, how stable is divalent tin?

Tin(II) fluorides and chloride fluorides have been handled in air in our laboratory for decades and they seem to be perfectly stable, provided heating is carried out under a non-reactive atmosphere (nitrogen or argon) in an inert container (Cu, Au or Pt) [2]. X-ray diffraction shows no change on aging in air at ambient temperature over long periods of time. However, it was observed that all polycrystalline samples of tin(II) studied in our laboratory show a weak broad Mössbauer absorption peak at 0 mm/s that can be explained only by the presence of a minor amount of SnO_2 that has to be amorphous since it is not observed by X-ray diffraction. For example, this is the case of SnF_2 and of $MSnF_4$ (M= Ba or Pb) [3, 4]. However, the Mössbauer spectrum of a large single crystal of $\alpha-SnF_2$, polished sufficiently thin enough to allow the $\gamma-$ray beam through and to avoid giving rise to line broadening by saturation, shows only the tin(II) doublet, with no SnO_2 peak at 0 mm/s [5]. Since the ratio surface/bulk is infinitely small in one single crystal compared to a powdered sample, it must be assumed that the small tin(IV) oxide peak observed in polycrystalline samples is due to surface oxidation of the particles, to give perhaps a monolayer, or a very small number of layers, such that the crystallites are too small to give rise to diffraction. For reactions of tin(II) compounds in aqueous solutions, it is extremely difficult to get the products free of tin(IV) [6, 7]. The purpose of the present work was to study the effect of heating stoichiometric tin(II) fluorides and more particularly study the stability of non-stoichiometric tin(II) fluorides and chloride fluorides at ambient conditions, and follow possible changes by X-ray powder diffraction and ^{119}Sn Mössbauer spectroscopy.

2 Experimental

2.1 Sample preparation

Monoclinic $\alpha-SnF_2$ (99 %) was purchased from Ozark-Mahoning. Crystals for structure determination were obtained by recrystallization in H_2O/HF. α-$PbSnF_4$ was prepared by adding dropwise a 1.700 M solution of $Pb(NO_3)_2$ to a 1.500 M solution of SnF_2 upon

vigorous stirring for a molar ratio Pb/[Pb+Sn] = 0.20. The $Ca_{1-x}Sn_xF_2$ solid solution was prepared by adding a 1.500 M solution of $Ca(NO_3)_2$ to a 1.500 M solution of SnF_2 for the ratio Ca/[Ca+Sn] $\geq$ 0.63.

The following phases in the SnF_2/PbF_2 system were prepared by heating the appropriate stoichiometric mixtures of $\alpha-SnF_2$ and of $\alpha-PbF_2$ at the given temperatures, in sealed copper tubes under nitrogen, according to the method designed by Dénès [2]: $\alpha-PbSnF_4$ (250 °C), $\beta-PbSnF_4$ (400 °C $\leq$ T $\leq$ 500 °C, followed by fast quenching in cold water), $PbSn_4F_{10}$ (250 °C, followed by fast quenching in cold water), the $Pb_{1-x}Sn_xF_2$ solid solution (0 $\leq$ x <0.50) (400 °C $\leq$ T $\leq$ 500 °C). The synthesis of $BaSnF_4$ was carried out by heating a stoichiometric mixture of $\alpha-SnF_2$ and BaF_2 in the same conditions as for the preparation of β-$PbSnF_4$.

The barium tin(II) chloride fluorides were prepared as follows:

– in aqueous medium: a 1.274 M solution of $BaCl_2.2H_2O$ was added to a 1.500 M solution of SnF_2 (labeled Ba $\rightarrow$ Sn on figures), or the solution of SnF_2 was added to the solution of $BaCl_2.2H_2O$ (Sn $\rightarrow$ Ba on figures). The molar ratio X of barium chloride in the reaction mixture is defined as follows: $X = n_{Ba}/[= n_{Ba} + n_{Sn}]$, where n_{Ba} is the number of moles of $BaCl_2.2H_2O$ and n_{Sn} is the number of moles of SnF_2. X was varied from 0.10 to 0.90 by increments of 0.10 for a course screening. Then, it was varied with a smaller increments around the X values of interest The following new compounds were obtained by this method:
  - $BaSn_2Cl_2F_4$: 0.34 $\leq$ X $\leq$ 0.40;
  - $BaSnClF_3.0.8H_2O$: 0.52 $\leq$ X $\leq$ 0.80;
  - the $Ba_{1-x}Sn_xCl_{1+y}F_{1-y}$ doubly disordered solid solution: X $\geq$ 0.85

The $Ba_{1-x}Sn_xCl_{1+y}F_{1-y}$ doubly disordered solid solution was also prepared by direct reactions in Cu tubes according to the method published by Dénès [2], at temperatures varying from 350 °C to 800 °C.

All syntheses from aqueous solutions were carried out under vigorous stirring, and resulted in a precipitate that was filtered immediately after the end of addition of the reactant in the burette. Then the precipitate was washed with a minimum of cold water and allowed to dry in air at ambient temperature. Any alteration of these conditions of preparation resulted in other compounds being formed, often in appreciable amounts.

2.2 X-ray powder diffraction

X-ray powder diffraction was used to identify of each crystalline phase and ensure that no crystalline impurity is contained in the samples. The samples were ground to a fine powder, although not overground, in order to avoid generating microcrystallinity/nanocrystallinity or phase transitions, as we have observed this to occur in some of these tin(II)-containing fluorides that have quite a soft lattice [8].

The X-ray powder diffraction patterns were collected on an Advanced Diffraction powder diffractometer from Scintag, Inc. instruments, using the K_α line of copper (λ = 1.54178 Å). Data accumulation was carried out by the DMNST software package from Scintag. The SIE112 software from Sietronics was used to process data. Search matches to compare phases obtained in this experiment with the JCPDS database were done using the $\mu-$PDSM software package®from Fein-Marquat. In addition, comparison was also done with our in-house library of diffraction patterns of the new phases prepared in our laboratory.

2.3 ^{119}Sn Mössbauer spectroscopy

The polycrystalline Mössbauer samples used for ambient temperature or low temperature measurements were intimately mixed and ground with sugar in order to have a sample with homogeneous Mössbauer thickness and to help randomize the orientation of the crystallites. For high temperature measurements, the samples were mixed with amorphous carbon. Highly oriented samples of α-$PbSnF_4$ were collected in the form of large thin platelets by suction filtration, using a Buchner funnel specially built for the experiment in such a way that the sample could be collected without disturbing the parallel alignment of the platelets. Homemade aluminum sample holders equipped with a very thin window were used for low temperature measurements, while PTFE (Teflon®) holders were used at high temperature. Low temperature spectra were collected using a APD Cryogenics closed cycle helium refrigerator operating at 16 K. The Mössbauer spectra were collected using a nominally 25 mCi $Ca^{119m}SnO_3$ source purchased form Ritverc. The detector was a scintillation counter from Harshaw fitted with a 1 mm thick (Tl)NaI crystal. A Pd foil was used to absorb the 25.04 keV and 25.72 keV X-ray lines generated by the source decay from the metastable 11/2 spin level of the ^{119m}Sn precursor to the 3/2 spin level excited state of interest. The Doppler velocity (-8 to +8 mm/s) was obtained by use of a an Elscint driving system including a MVT-4 velocity transducer, a MDF-N-5 waveform generator and a MFG-N-5 driver. The data were accumulated in a Tracor-Northern TN 7200 multichannel analyzer that has a built-in amplifier and a single channel analyzer. The spectra were evaluated using the GMFP5 software [9], that is an extension to the GMFP software to five sites [10].

3 Results and discussion

3.1 Tin electronic structure, bonding type, coordination and Mössbauer spectrum

Tin, atomic number $Z = 50$, belongs to group 14 / period 5 of the periodic table. It has four valence electrons and its electronic structure is [Kr] $4d^{10}\ 5s^2\ 5p^2$. Squeezed between the metalloid germanium and the weak metal lead, it is a very weak metal. Indeed, on cooling below 13.2 °C, it undergoes a metal → diamond structural phase transition (http://en.wikipedia.org/wiki/Tin). This makes that most of its chemistry is covalent.

In its compounds, it is commonly found in both the +4 full oxidation state and in the +2 suboxidation state. In the latter case, two of the valence electrons remain in the valence shell and are not used for bonding. Such pairs of electrons not used for bonding are called *"lone pairs"* or "*non-bonded electron pairs*." This can result in two situations:

a. The Sn^{2+} ion is formed. This situation is found mostly with large weakly electronegative metalloids or non-metals, such as selenium, tellurium and iodine, and in some cases bromine. In this situation, the Sn^{2+} electronic structure is [Kr] $4d^{10}\ 5s^2$, i.e. the tin lone pair remains on the native *5s* orbital. Bonding is ionic and the tin orbitals are not hybridized. Since *s* orbitals are spherical, the lone pair being purely $5s^2$ makes the stannous ion spherical, therefore its coordination can be highly symmetrical, like tetrahedral, octahedral or cubic. Small distortions can occur, as allowed by local crystal symmetry. When the stannous ion is present, the lone pair is said to be "*non-stereoactive*", since being on an unhybridized spherical orbital, it does not modify the stereochemistry, i.e. it does not modify the tin coordination [11].

b. Tin(II) is covalently bonded. This is found for small and highly electronegative nonmetals, such as fluorine, chlorine, oxygen sulfur and most of the time bromine. In this bonding mode, the tin valence orbitals are hybridized. The following types of hybridization schemes have been observed, where the lone pair E occupies one of the hybrid orbitals:

   – sp^3: tetrahedral electron pair geometry, trigonal pyramidal molecular geometry, SnX_3E, similar to the NH_3 molecule;
   – sp^3d: trigonal bipyramidal electron pair geometry, see-saw molecular geometry, SnX_4E, similar to SF_4;
   – sp^3d^2: octahedral electron pair geometry, square pyramidal molecular geometry, SnX_5E, similar to ClF_5.

In all of the above cases, the geometry is in agreement with the expectations of the *Valence Shell Electron Pair Repulsion* (VSEPR) model of Gillespie and Nyholm [12]. The VSEPR model accounts for the molecular geometry in nearly all cases for main group elements in free molecules. Deviations are observed in solids because of the contribution from the lattice energy. For example, in SnO and red PbO, the coordination MO_4E is square pyramidal, instead of see-saw expected by the VSEPR model [11, 13]. Being located on a hybrid orbital, a stereoactive lone pair occupies a position in the valence shell of the tin atom that would otherwise be occupied by a bonding pair, connected to an atom in the tin sphere of coordination. Therefore, a stereoactive lone pair decreases the coordination number by at least one. In addition, in agreement with the VSEPR model, a lone pair occupies more room in the valence shell of an atom than a bonding pair, therefore lone pair – bonding pair repulsions are larger than the repulsion between two bonding pairs, and it results an additional distortion of the polyhedron of coordination of covalently bonded tin, making the bond angles smaller.

Tin-119 has a nuclear spin system of 1/2 in the ground state and 3/2 in the first excited state. Since tin is diamagnetic in all its stable oxidation states (+2 and +4), there is no magnetic hyperfine splitting, in the absence of a transferred field or an applied field. Line splitting can occur only due to quadrupolar interactions. Since the nucleus of spin 1/2 has no quadrupole moment, only the first excited state splits in an electric field gradient (e.f.g.). In the latter case, the excited state splits to two sublevels, $|1/2>$and $|3/2>$, and therefore two transitions, $|1/2> \rightarrow |1/2>$and $|1/2> \rightarrow |3/2>$take place (Fig. 1).

The probability of the two transitions is the same in randomly oriented polycrystalline samples. It should therefore result in a symmetric doublet. However, in divalent tin compounds, the doublet is often asymmetric, and in some cases, a single line is observed.

3.2 The small tin(IV) peak at ≈ 0 mm/s in tin(II) compounds

The Mössbauer spectrum of nearly all divalent tin compounds shows, in addition to the tin(II) singlet or doublet, a small peak at ca. 0 mm/s that is representative of tin(IV) surrounded by oxygen. This is, for example, the case of $\alpha-SnF_2$ (Fig. 2). The ambient temperature spectrum is a doublet at $\delta = 3.430(1)$ mm/s and $\Delta = 1.532(1)$ mm/s [3]. This is in agreement with the molecular structure of $\alpha-SnF_2$ (Fig. 3) [14]. The small increase of isomer shift at low temperature is due to the second order Doppler shift. The doublet asymmetry at ambient temperature is due to the Goldanskii-Karyagin effect and it vanishes at very low temperature, as expected, when thermal vibrations are frozen [15]. In addition to the strong tin(II) doublet, a small tin(IV) peak at ca. 0 mm/s is present. It shows that

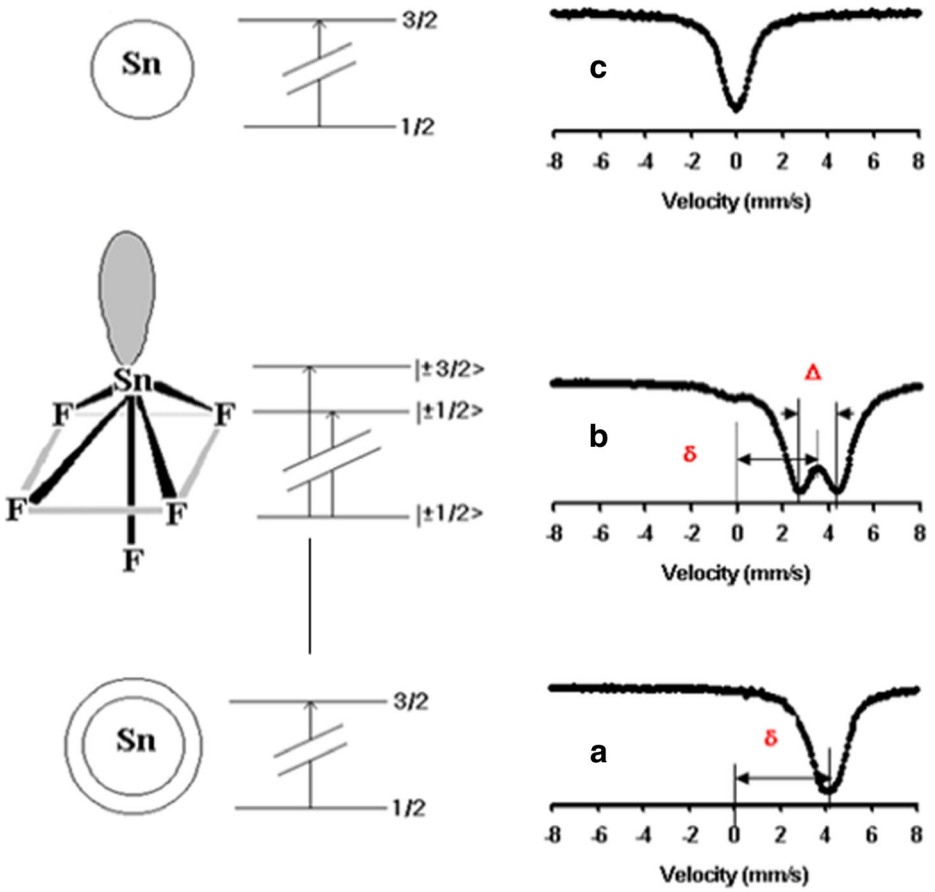

Fig. 1 Mössbauer spectra for **a** Ionic Sn^{2+}, **b** Covalently bonded tin(II) in $BaSnF_4$, and **c** $CaSnO_3$

the sample contains a small amount of a species that has Sn(IV)-O bonds. This is surprising since the sample was prepared by grinding small crystals of $\alpha-SnF_2$ that should not contain impurities, and X-ray powder diffraction shows only $\alpha-SnF_2$. The impurity can be attributed to SnO_2, that has to be amorphous, since it is not detected by X-ray powder diffraction. It is logical to suppose that it is due to surface oxidation of the particles. This hypothesis is reinforced by the fact that the spectrum of a single crystal of $\alpha-SnF_2$, glued to a thin sheet of aluminum, thin enough to allow enough of the $\gamma-$ray beam through, that had been polished to be thin enough to avoid absorbing an excess amount of the $\gamma-$ray beam and to avoid line broadening, shows no trace of the SnO_2 peak at 0 mm/s [5]. This experiment proves that the SnO_2 is a surface oxidation of the particle since the ratio surface/bulk increases with decreasing particle size, and it is nearly infinitely small in a single crystal.

Using the measured thickness of the single crystal, 0.31(5) mm, and the computed value for the thickness, *Ta*,, the recoil-free fraction of $\alpha-SnF_2$ was estimated to be 0.034 at ambient temperature, in good agreement with a previously reported values [16]. In contrast, the recoil-free fraction of SnO_2 can be expected to be much higher, around 0.6 like in $BaSnO_3$

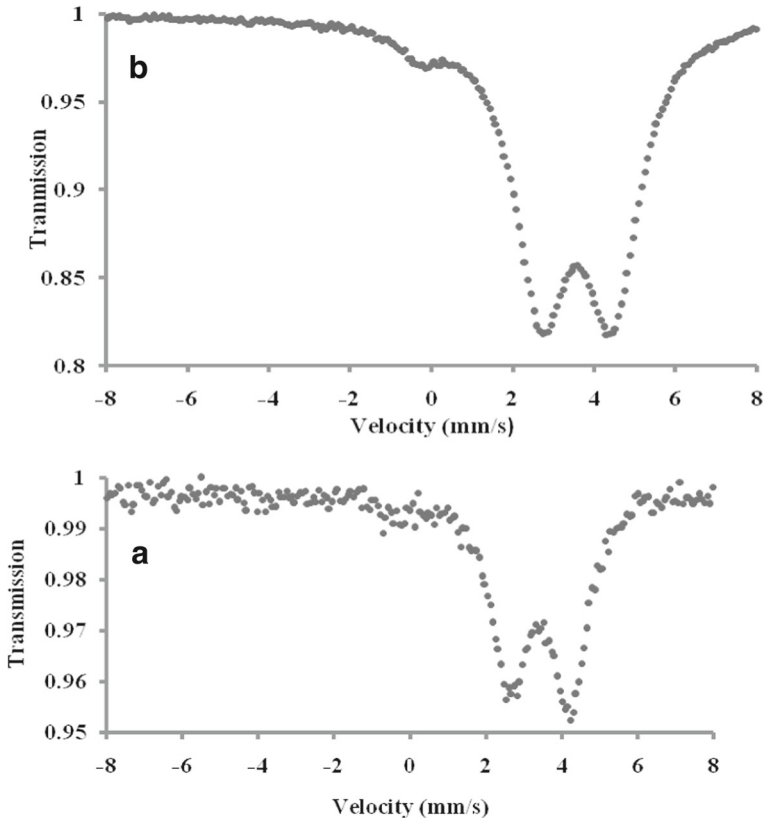

Fig. 2 ^{119}Sn Mössbauer spectrum of $\alpha-SnF_2$: **a** at ambient temperature, **b** at 12.5 K

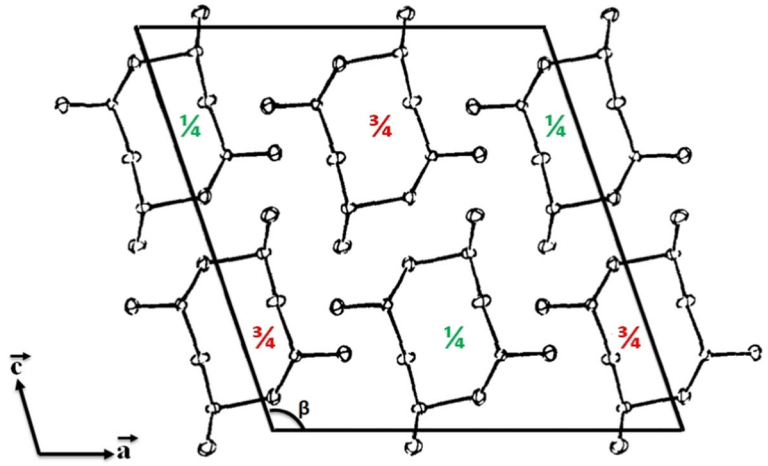

Fig. 3 The crystal structure of $\alpha-SnF_2$ consists of Sn_4F_8 tetramers. The Sn-F bonds are covalent. The numbers 1/4 and 3/4 are the *y* coordinate of the average height of each tetramer

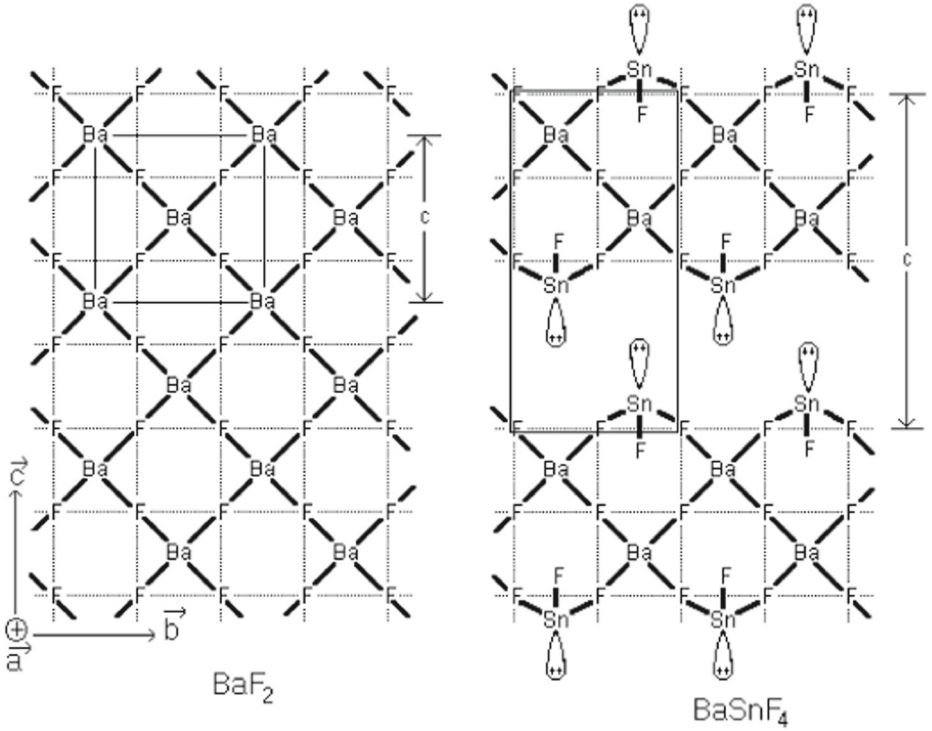

Fig. 4 Projection of a slice of the structure of BaF_2 and $BaSnF_4$ on the (a, b) plane in the BaF_2 axes

[17]. Indeed, the Debye temperature of SnO_2 must be much higher than that of SnF_2 since bonding is much stronger in the former, due to the following:

- the product of the ionic charges in Coulomb's law for estimating the energy of each bond is -8e (e = charge of the proton) in SnO_2 while it is only -2e in SnF_2. In addition, the distance Sn(IV)-O <Sn(II)-F in the denominator of Coulomb's law;
- SnO_2 crystallizes in the rutile structure, This is a compact structure, with a distorted octahedron of oxides ions around each tin(IV), while the coordination number of tin is three for Sn(1) and five for Sn(2) in $\alpha-SnF_2$, since the stereoactive lone pair pushes away one fluorine atom (for Sn(2)) or three (for Sn(1)), thereby reducing the coordination number and increasing the softness of the structure [14]. This can be seen by the dramatic difference of their melting points, 215 °C for SnF_2 [18] and 1,360 °C [19] for SnO_2. It results that the recoil-free fraction of SnO_2 is about 20 times as high as that of SnF_2, thereby making the SnO_2 Mössbauer peak about 20 times stronger than the peaks of SnF_2 at equal amount of the two compounds. Therefore, the relative intensity of the SnO_2 peak gives false impression that the amount of SnO_2 in the sample is much larger than what it really is.

3.3 Passivation of tin-rich fluorides and chloride fluorides

The structure of $BaSnF_4$ is a two-dimensional and ordered structure and a $(a/\sqrt{2}, a/\sqrt{2}, 2c)$ superstructure of the fluorite-type structure of $BaSnF_4$ (Fig. 4). The Mössbauer spectrum

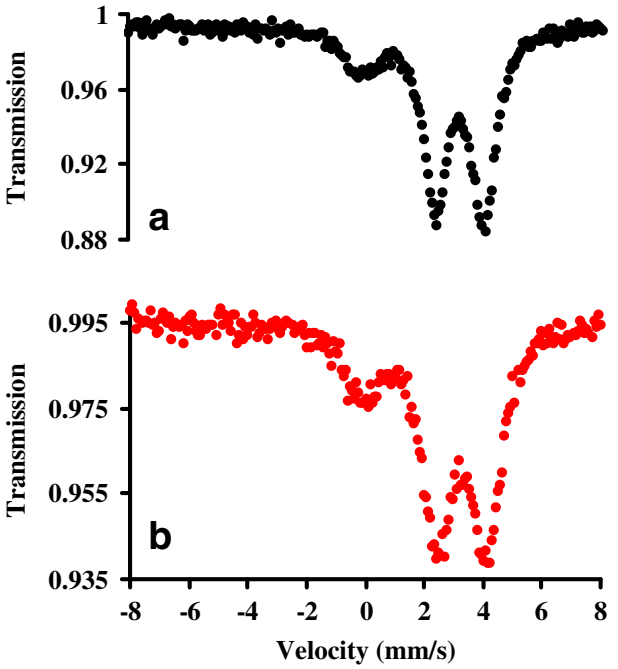

Fig. 5 Room temperature tin-119 Mössbauer spectrum of $BaSnF_4$ prepared by reaction in dry conditions at 500 °C for 2 hours under nitrogen **a** young, and **b** aged for 69 months. Note: The weaker total absorption after aging is due to the fact that the amount of sample used was lower

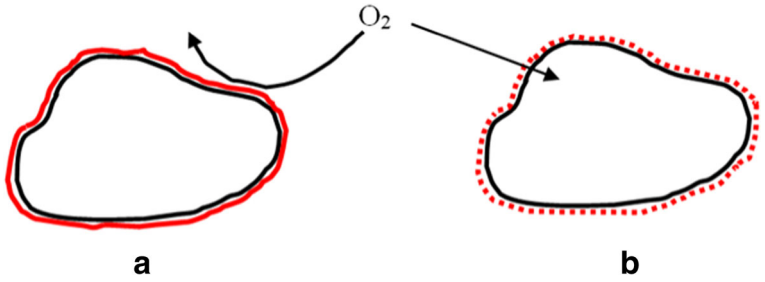

Fig. 6 Influence of SnO_2 surface layer continuity on the efficacy of passivation: **a** passivating layer of SnO_2 (full coverage) in fluorides rich in tin, **b**: Non-passivating incomplete layer of SnO_2 (partial coverage) in $Ba_{1-x}Sn_xCl_{1+y}F_{1-y}$

of a sample was run when young and after exposure to air at ambient temperature for over three years (Fig. 5). No significant increase of the relative intensity of the SnO_2 peak is observed. This seems to indicate that there is an initial oxidation of a minor amount on the divalent tin to give SnO_2, and then, this process stops, probably because the stannic oxide formed initially protects against further oxidation. In order to do that, the SnO_2 formed would have to be present in the form of a protective layer at the surface of the particles (Fig. 6a), similar to a layer of paint or varnish and to the passivating layer of alumina on the surface of aluminum metal that protects against further corrosion. The hypothesis of a

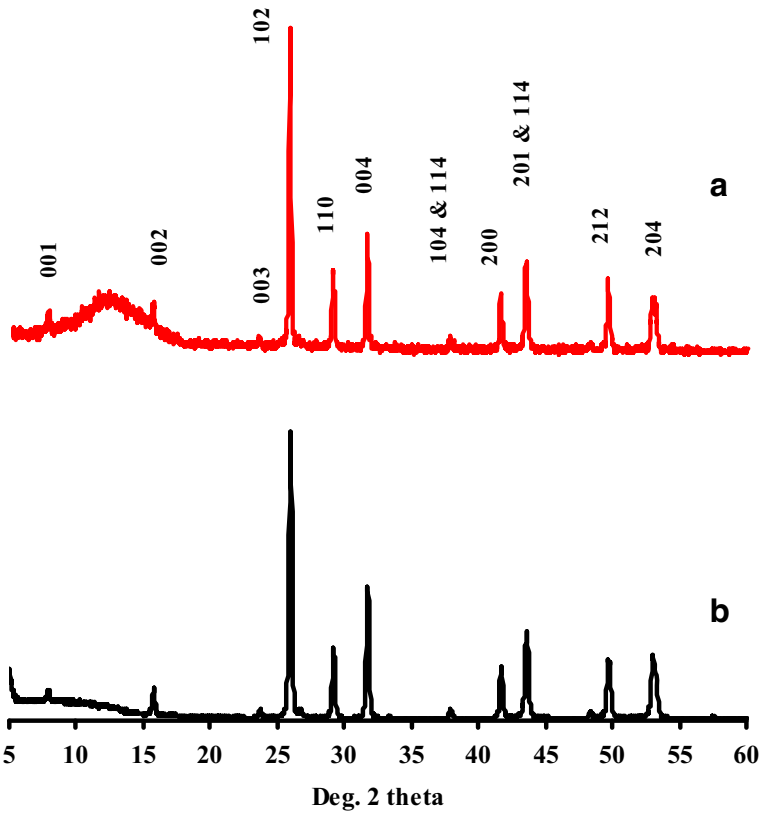

Fig. 7 Room temperature X-ray powder diffraction pattern of $BaSnF_4$ prepared by direct reaction at 500 °C for 2 hours **a** young, and **b** aged for 69 months

very thin layer of SnO_2 at the surface of the particles is reinforced by the fact that no SnO_2 is observed by X-ray diffraction (Fig. 7). The same X-ray powder diffraction is observed before and after aging, with all peaks being indexed in the tetragonal unit-cell of $BaSnF_4$. The lack of SnO_2 peaks shows that there is too little of it and/or the crystallites are too small to give rise to diffraction.

When $BaSnF_4$ was heated at 100 °C , there was an initial increase of the tin(IV) peak, and then its growth stops while heating at constant temperature. A further initial increase of the tin(IV) peak occurred at 200 °C, and it stops again upon further heating at the same temperature (Fig. 8). This shows that passivation breaks down when temperature increases. This is not surprising: higher thermal vibrations weaken bond and increase the reactivity. This results in a thickening of the SnO_2 layer, that restores passivation. Of course, this mechanism works less and less well as temperature is increased.

3.4 Passivation of solid solutions of fluorides poor in tin(II)

CaF_2 and PbF_2 form $M_{1-x}Sn_xF_2$ solid solutions. Their X-ray diffraction patterns (Fig. 9a−2) is the same as that of the parent MF_2 compound (Fig. 9a−1), with some small

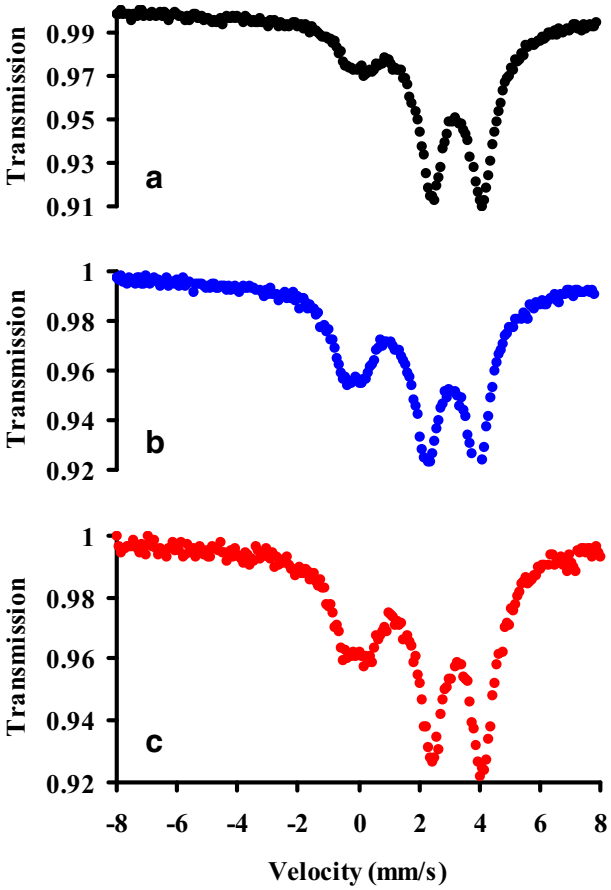

Fig. 8 Ambient temperature tin-119 Mössbauer spectrum of $BaSnF_4$: **a** unheated; **b** heated for 23 hrs in air at 100 °C, **c** heated for 21 hrs in air at 200 °C

line shit due to the size difference between the M^{2+}cation and tin(II), and a significant amount of line broadening for $Ca_{1-x}Sn_xF_2$ that shows the sample is nanocrystalline. The absence of superstructure reflections and of line splitting shows that tin and the other metal are fully disordered on the M^{2+} site (*positional disorder*). Therefore, tin(II) should have the same cubic coordination as M^{2+}, therefore it should have a non-stereoactive lone pair and unhybridized orbitals, and form ionic bonding. This would give the Mossbauer spectrum of Fig. 1a, i.e. a single line at ca. 4 mm/s. However, Figs. 9b-2 and 10b are clearly large quadrupole doublets at high isomer shift similar to Fig. 1b, characteristics of covalently bonded tin(II) with a stereoactive lone pair on a hybrid orbital. Since the tin-lone pair axis defines a special direction locally, the special directions of all the tin atoms must be disordered relative to one another (*orientational disorder*) in order to preserve the overall cubic symmetry of the crystal lattice observed by X-ray diffraction (Fig. 11).

It should be noted on Figs. 9b-2 and 10b that the SnO_2 peak is as small for the $M_{1-x}Sn_xF_2$ solid solutions than for the ordered fluorides, SnF_2 or $BaSnF_4$ (Figs. 2 and 5).

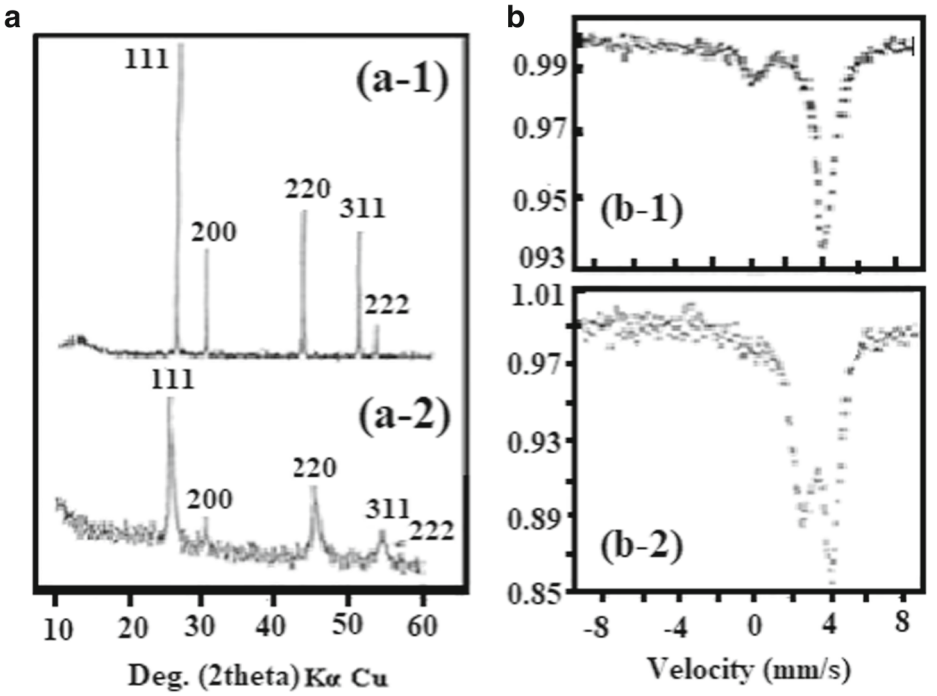

Fig. 9 **a** X-ray powder diffraction pattern of: (a-1) CaF_2 and (a-2) $Ca_{1-x}Sn_xF_2$ (x = 0.27), **b**: ^{119}Sn ambient temperature Mössbauer spectrum of: (b-1) $Ba_{1-x}Sn_xCl_{1+y}F_{1-y}$ (x = 0.15, y = 0.094) and (b-2) $Ca_{1-x}Sn_xF_2$ (x = 0.27)

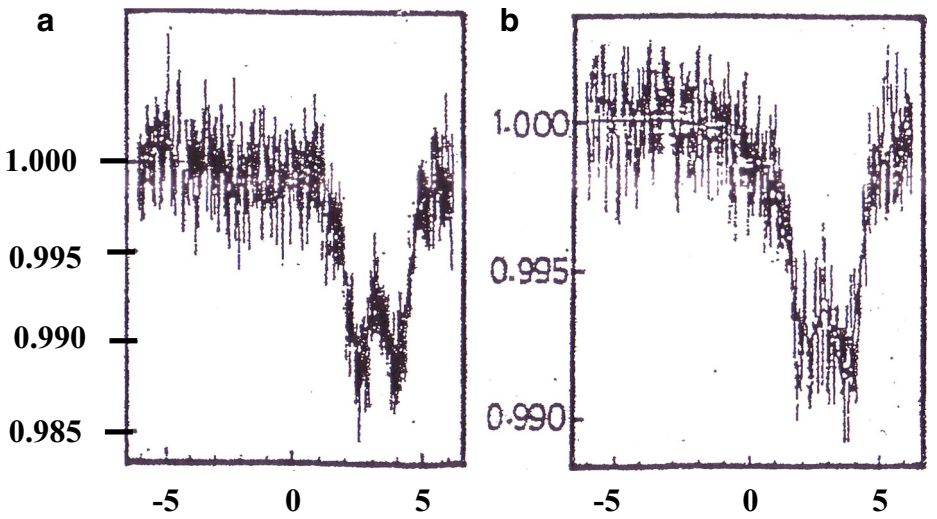

Fig. 10 Ambient temperature ^{119}Sn Mössbauer spectrum of **a** β-$PbSnF_4$ and **b** $Pb_{0.70}Sn_{0.30}F_2$

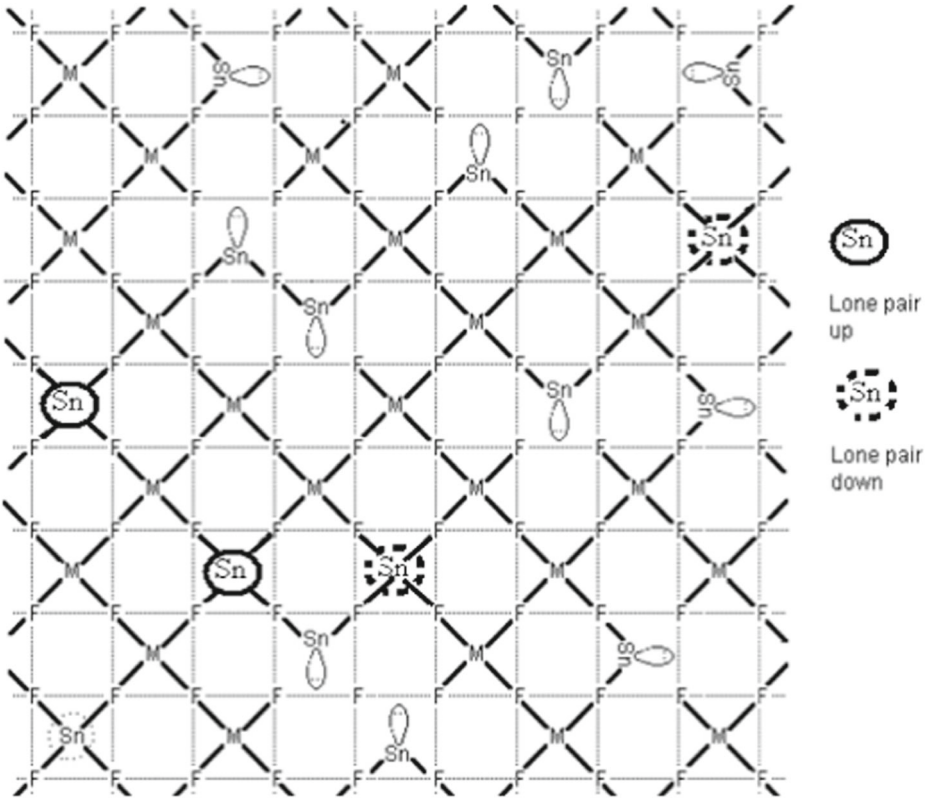

Fig. 11 Projection of a structural model of the disordered M/Sn/F phases: M and Sn are randomly distributed in the $[F_8]$ cubes (*positional disorder*) the tin lone pair points randomly towards any of the six faces of the $[F_8]$ cubes (*orientational disorder*)

This means that passivation is as efficient in the solid solutions despite the low tin content, low enough to make it impossible to have full coverage by a protective layer of SnO_2 as shown on Fig. 6a. Instead, a discontinuous coverage by fragments of SnO_2 should allow a significant amount of oxygen to reach the divalent tin and result in a highly inefficient passivation (Fig. 6b). One or more other factors must be important for regulating the phenomenon of passivation.

3.5 Variable degrees of passivation in tin(II) barium chloride fluorides

3.5.1 Samples prepared by precipitation

Precipitation from aqueous solutions of stannous fluoride SnF_2 and barium chloride $BaCl_2$ give rise to the precipitation of $BaSn_2F_6$ and three new barium tin(II) chloride fluorides. Two of these are stoichiometric: $BaSn_2Cl_2F_4$ and $BaSnClF_3.0.8H_2O$, while the other is a solid solution, the formula of which is better written as $Ba_{1-x}Sn_xCl_{1+y}F_{1-y}$ because, as shown by X-ray diffraction (Fig. 12), it has the BaClF structure [20–22]. The Mössbauer

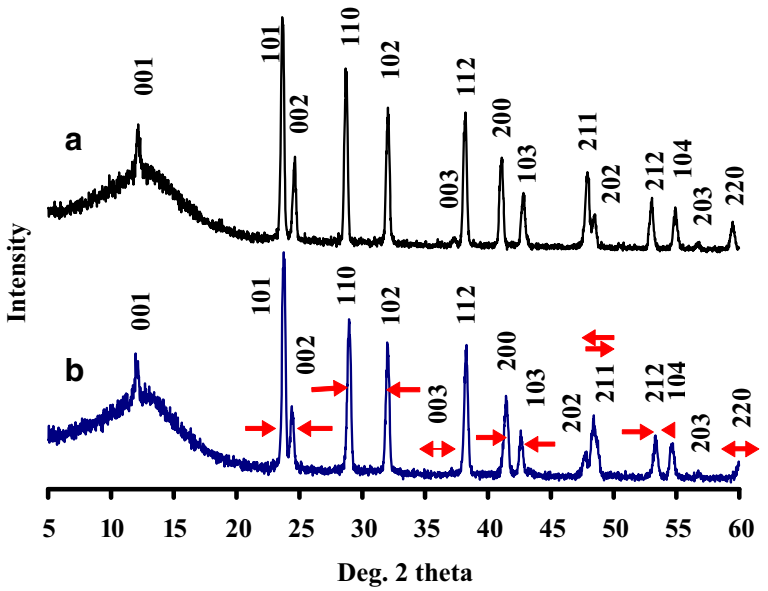

Fig. 12 X-ray diffraction pattern of **a**: unsubstituted BaClF (X = 1.00), **b**: substituted BaClF [$Ba_{0.85}Sn_{0.15}Cl_{1.11}F_{0.89}$ (X = 0.860, Sn → Ba)]

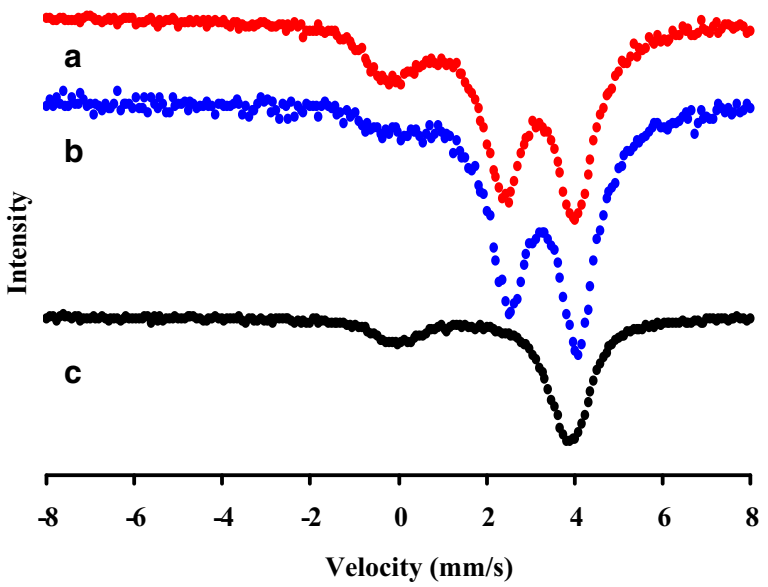

Fig. 13 Room temperature tin-119 Mössbauer spectrum of **a**: $BaSn_2Cl_2F_4$, **b**: $Ba_3Sn_3Cl_4F_8 \bullet 2H_2O$, (c): $Ba_{0.85}Sn_{0.15}Cl_{1.11}F_{0.89}$

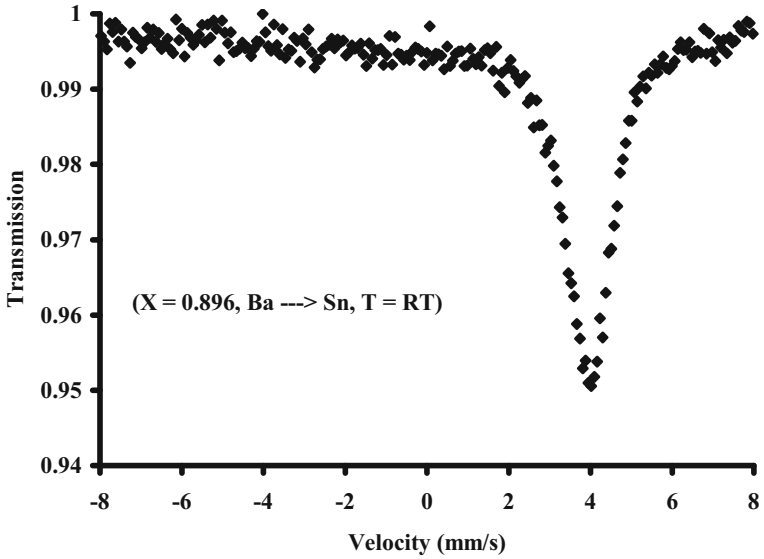

Fig. 14 Ambient temperature ^{119}Sn Mössbauer spectrum of precipitated $Ba_{1-x}Sn_xCl_{1+y}F_{1-y}$ at ambient temperature at X = 0.896, for Ba→ Sn

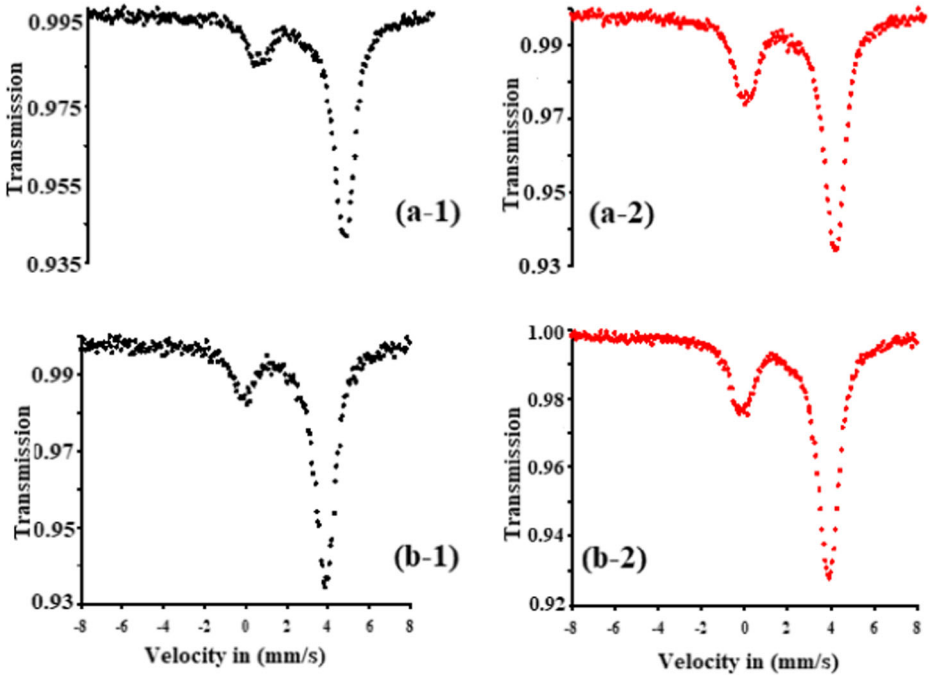

Fig. 15 Ambient temperature ^{119}Sn Mössbauer spectrum of precipitated samples (a-1 & a-2) X = 0.850, Ba → Sn, $Ba_{1-x}Sn_xCl_{1+y}F_{1-y}$, aged for 18.00 m (a-1) and 27.00 m (a-2), and (b-1 & b-2) X = 0.855, Ba → Sn, $Ba_{1-x}Sn_xCl_{1+y}F_{1-y}$ aged for 2.50 m (b-1) and 45.00 m (b-2). Note: the unit of age *m* means months

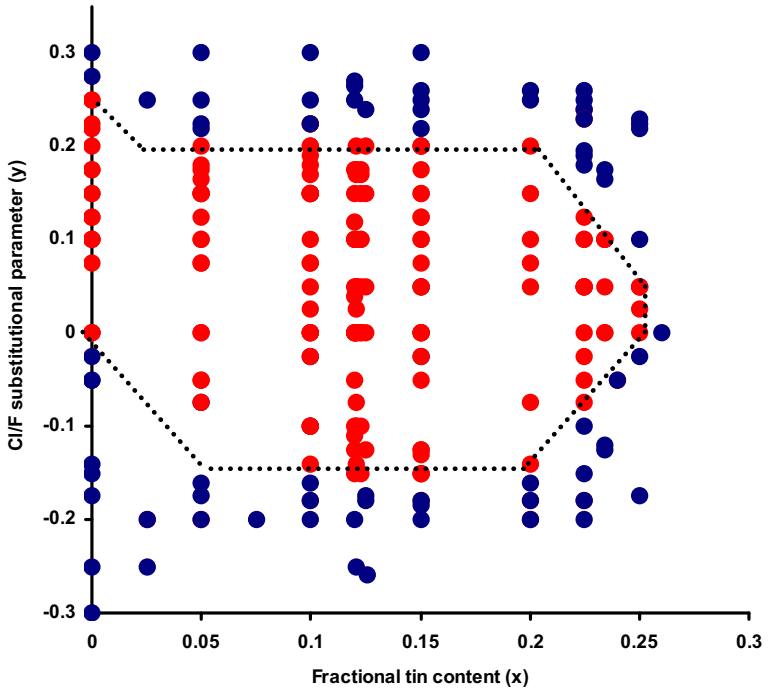

Fig. 16 Diagram of the $Ba_{1-x}Sn_xCl_{1+y}F_{1-y}$ solid solution in the (x, y) plane, obtained by reaction at 350 °C for 43 hours, ● pure $Ba_{1-x}Sn_xCl_{1+y}F_{1-y}$ phase and ● mixture of $Ba_{1-x}Sn_xCl_{1+y}F_{1-y}$ with other phases

spectra of Fig. 13 for the three barium tin(II) chloride fluorides obtained by precipitation show a large quadrupole doublet typical of covalent bonding for the two stoichiometric compounds, while the solid solution has a significantly broadened line close to 4 mm/s characteristic of ionic bonding with a distorted environment of the Sn^{2+} ion. It should be noted that the three Mössbauer spectra show, in addition to the tin(II) lines, a weak line at ca. 0 mm/s characteristic of SnO_2, like in the fluorides and similarly, no increase of the tin(IV) line increases with age, therefore, passivation against further oxidation seems to be very efficient. However, in one occasion, the precipitated solid solution was found to be free of SnO_2 for no reason that could be identified (Fig. 14).

When the precipitated solution that contains SnO_2 at a young age is allowed to age for several years under air, the intensity of the SnO_2 peak increases slowly (Fig. 15). This shows that it does not passivate as efficiently as the fluorides or the stoichiometric chloride fluorides.

3.5.2 Samples prepared by high temperature reactions in dry conditions

Pure $Ba_{1-x}Sn_xCl_{1+y}F_{1-y}$ solid solution was obtained in a wide range of chemical compositions (Fig. 16). The Mössbauer spectrum of the solid solution changes dramatically with the values of the fractional amount x of tin substituting barium and versus the fractional

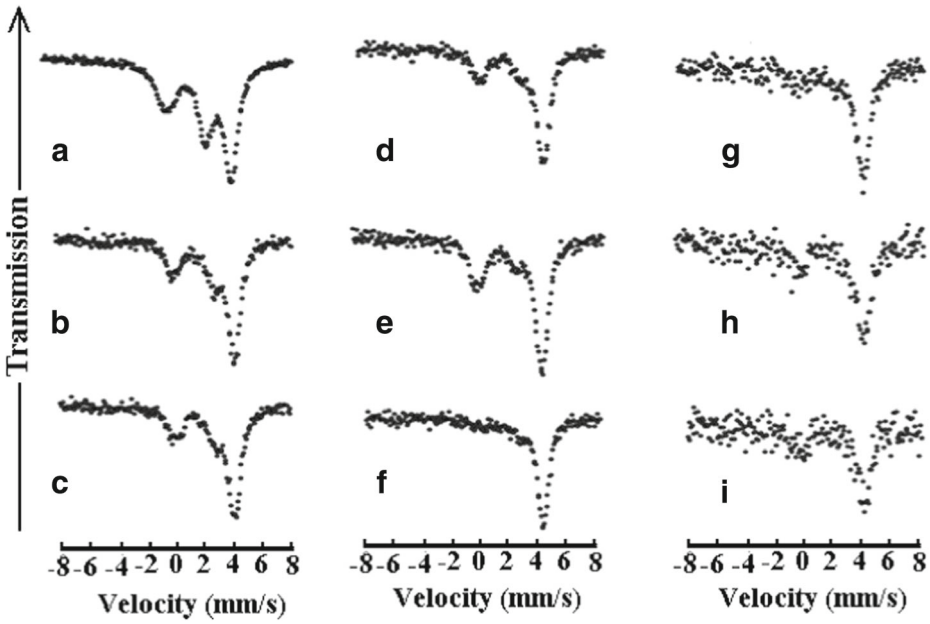

Fig. 17 Ambient temperature ^{119}Sn Mössbauer spectrum of $Ba_{1-x}Sn_xCl_{1+y}F_{1-y}$ solid solution prepared by direct reaction at 350 °C for 43 hours, x = 0.225, and **a**: y = −0.15, **b**: y = −0.10, **c**: y = −0.05, **d**: y = 0.00, **e**: y = 0.05, **f**: y = 0.10, **g**: y = 0.15, **h**: y = 0.20, **i**: y = 0.25. All samples contain the same amount of tin, the same amount of sample was used for each, and the data of spectra for y≥0.15 were collected for 15-20 days versus only 2 or 3 days for the others

amount y of fluorine substituting chlorine (if $y<0$) or of chlorine substituting fluorine (if $y>0$) (Fig. 17). For a constant value of x, bonding and lattice srength in the solid solution varies as follows:

- $y<0$ (excess F over Cl) (Fig. 17a): the highly asymmetric tin(II) doublet is actually a doublet (covalent bonding) overlapping with a singlet (ionic bonding). The strong signal shows that the recoil-free fraction is similar to that of ordered fluorides;
- y less negative (smaller excess of F) to $y = 0.10$ (small excess of Cl) (Fig. 17b to f): the doublet gets weaker and weaker while the single line becomes predominant, therefore there is less and less covalently bonded tin and more and more ionic bonding (Sn^{2+});
- $y = 0.15$ to 0.25 (increasing excess of Cl over F) (Fig. 17g to i): the single line at ca 4 mm/s shows that all the tin(II) is ionic. In addition, the signal becomes weaker and weaker, hence the recoil-free fraction becomes smaller and smaller.

This results in the following bonding model of the solid solution (Fig. 18):

(i) covalent Sn-F bonds are formed in systems at high x (rich in tin) and low y (rich in fluorine). There is a sufficient amount of Sn and F to form ... - F- Sn - F - Sn-F- ... oligomers with covalent bonding similar to stoichiometric fluorides, hence a similar bond strength that results in a similar recoil-free fraction (Fig. 18a).

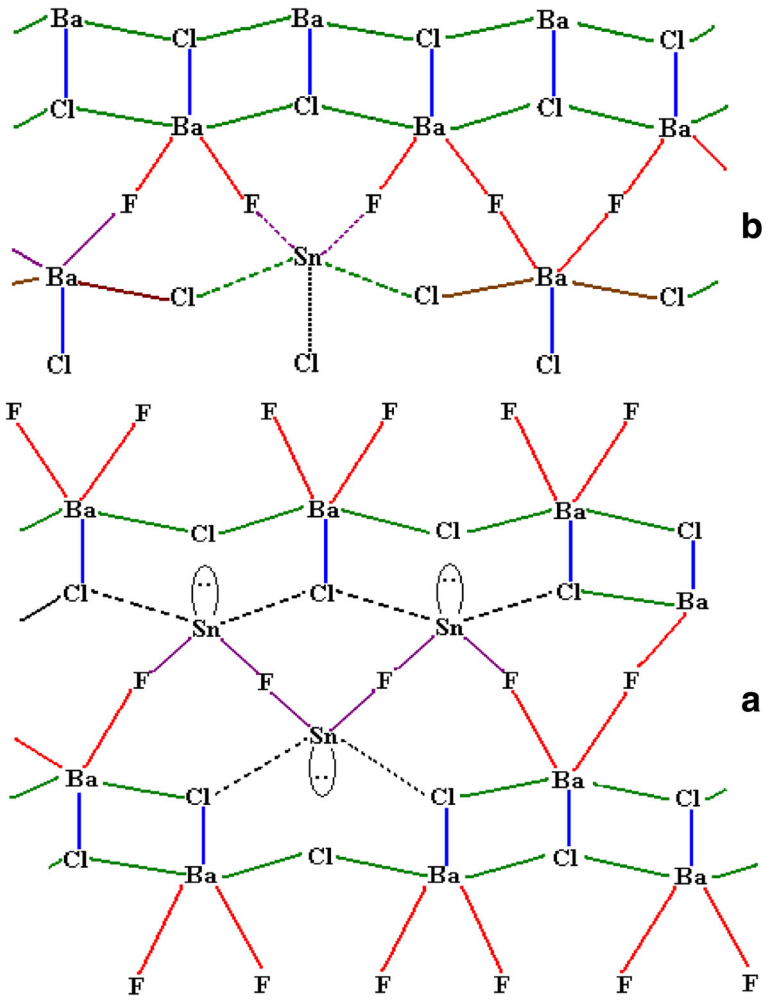

Fig. 18 Tin(II) bonding in $Ba_{1-x}Sn_xCl_{1+y}F_{1-y}$ for $\mathbf{y} = 0$: **a** clusters of covalently bonded tin in systems richer in tin and in fluorine, and **b** ionic bonding in systems dilute in tin and richer in chlorine

(ii) ionic bonding when x is low enough to make the probability of tin clustering low and y high enough to make each tin to be likely to be surrounded by a large number of Cl than F. In such a case, the Sn^{2+} ions replace the Ba^{2+} ions in the BaClF structure (Fig. 18b), and it results the following:

- Since tin is present in the form of Sn^{2+} ions, the Mössbauer spectrum is a single line at ca. 4 mm/s;
- since there is much more barium ions than tin(II) ions in the structure, the ionic lattice is basically the same as for unsubstituted BaClF with the cationic sites having a size very similar to that of a Ba^{2+} ion, and since the Ba^{2+} ion is much

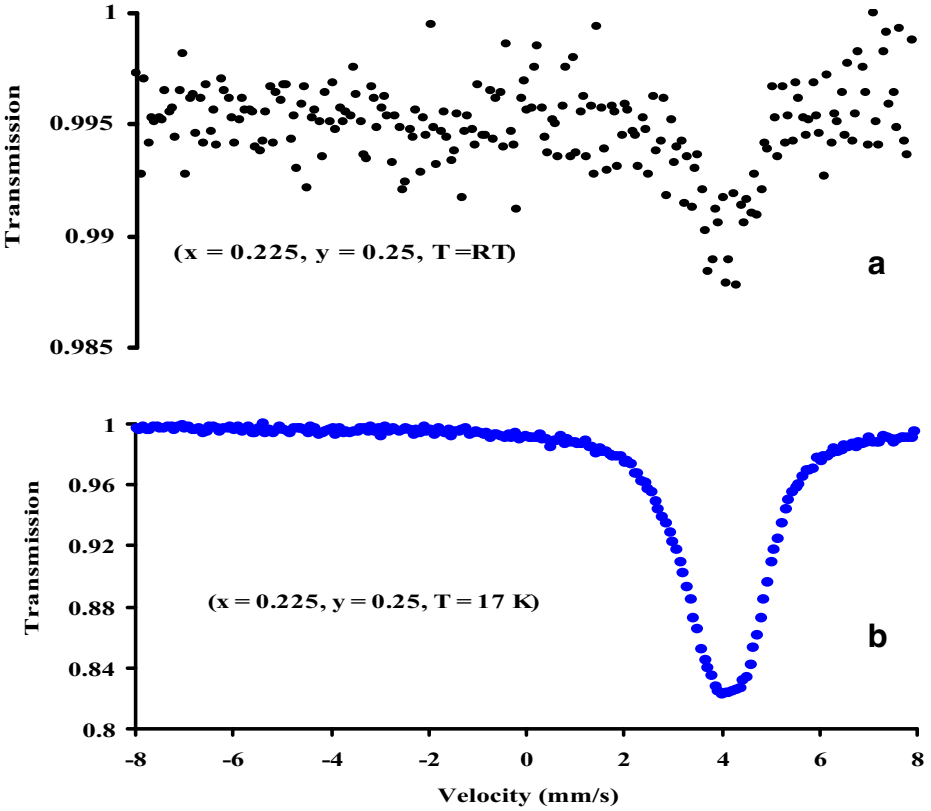

Fig. 19 ^{119}Sn Mössbauer spectrum of a sample obtained by the dry method for $x = 0.225$, $y = 0.250$, **a**: at 298K, and **b**: at 17K. The same sample (same amount of tin) was used for the two temperatures. Data accumulation time, with the same γ−ray source, was 3 weeks for spectrum (**a**) and 2 days for spectrum (**b**)

bulkier than the Sn^{2+} ion [23], the stannous ion is located in a highly oversized site, and in addition, if there is an excess of Cl over F, and Sn-Cl bonds are weaker than Sn-F bonds, Sn^{2+} forms no significant amount of bonding to the surrounding anions and it rattles in its oversized anionic box, hence a very low recoil-free fraction results, as can be seen by the weaker and weaker Mössbauer line as the amount of Cl increases at the expenses of F (Fig. 17g to i). Collecting the spectrum of Fig. 17i at 17 K resulted in a very strong spectrum, with the absorption at the peak maximum increasing by a factor of about 3,400 % (Fig 19). This shows that the rattling freezes at very low temperature, and that indeed, tin bonds are infinitely weak a ambient temperature.

The spectrum of Fig. 19 shows nearly no detectable amount of SnO_2, because it was freshly prepared and protected from exposure to air. Once the solid solution with ionic bonding is exposed to air, the amount of SnO_2 increases more rapidly than for the covalently bonded fluorides, and it keeps increasing, in other words, passivation does not seem to work well (Fig. 20).

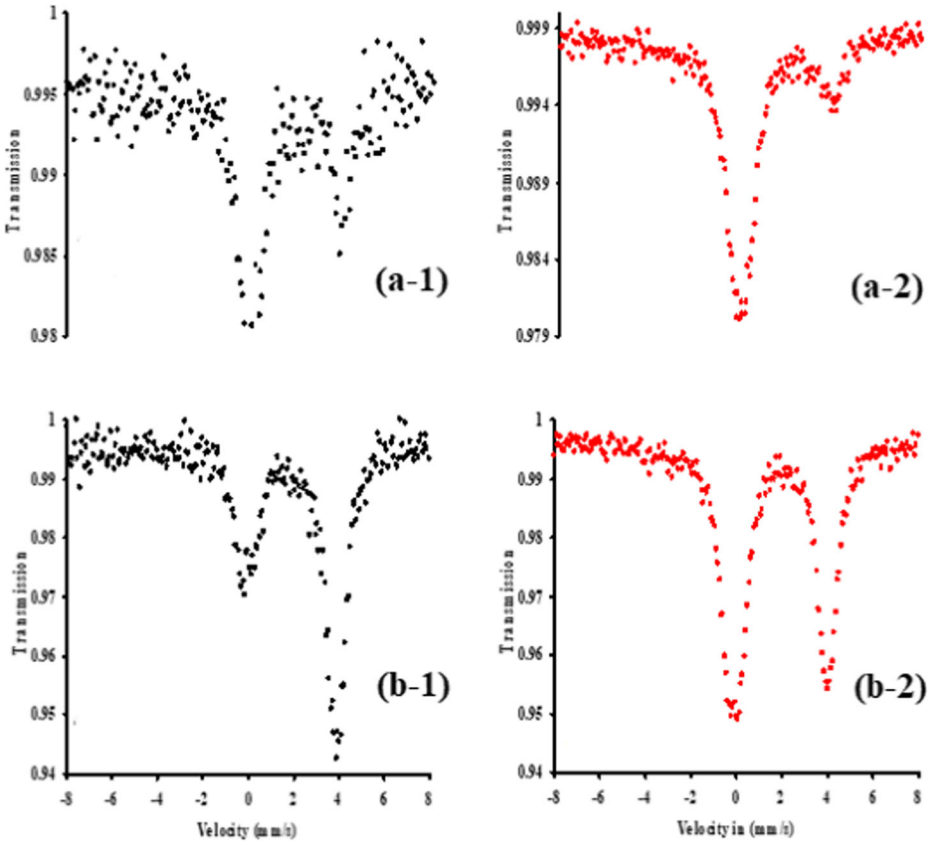

Fig. 20 Ambient temperature ^{119}Sn Mössbauer spectrum of the $Ba_{1-x}Sn_xCl_{1+y}F_{1-y}$ solid solution prepared by the dry method (freshly prepared and aged): (a-1 & a-2), x = 0.050, y = 0.100 (freshly prepared (a-1) and aged for 32 months (a-2), (b-1 & b-2) x = 0.121, y = 0.000 (freshly prepared (b-1) and aged for 36.7 months (b-2)

The relative amount of SnO_2 signal on aging is hard to predict or to control, however the following trends were observed:

(i) The more SnO_2 there is at a young age, the faster the growth of the amount of SnO_2 on aging (Fig. 21). This shows that when tin(II) bonding to its surrounding is weak, oxidation starts early at a young age and keeps taking place as time goes on.

(ii) When the percentage increase of SnO_2 per month is plotted versus the intensity of the 4 mm/s peak (Sn^{2+} peak), it is obvious that ionic Sn^{2+} tin oxidizes much faster than covalently bonded tin(II) (Fig. 22).

(iii) When the percentage tin(IV) signal increase per month is plotted versus the total % tin(II) (ionic + covalent) absorption at age zero (Fig. 23), four regions are observed: A: low *Sn*, medium f_a, B: low *Sn*, high *Cl* (i.e. low*F*), C: high *Sn*, high *Cl* (i.e. low *F*), instability, D: high *Sn*, low *Cl* (i.e. high F), high f_a. The main observation to be obtained from this plot is that the lower the tin(II) recoilless fraction, the

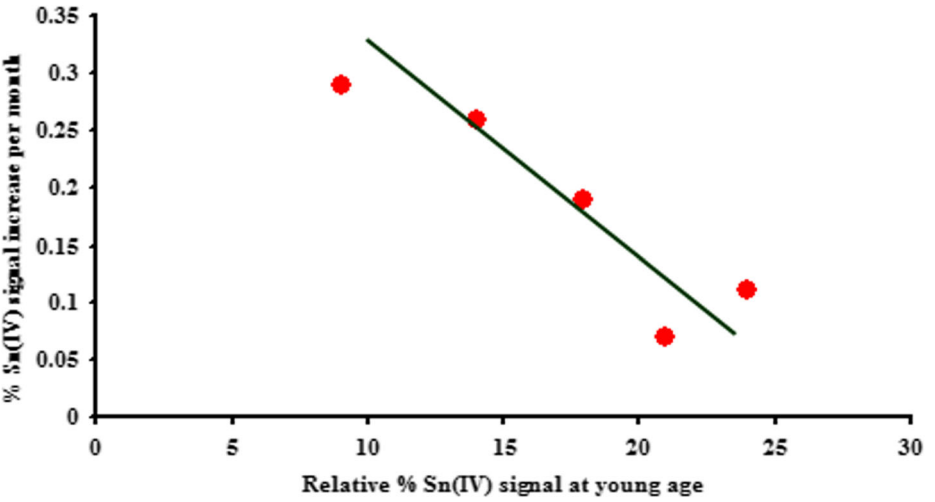

Fig. 21 Percentage increase of the tin(IV) signal relative to the total Sn per month, versus the relative % signal Sn(IV) at a young age. The line is just a guide for the eye. It was not fitted to any model

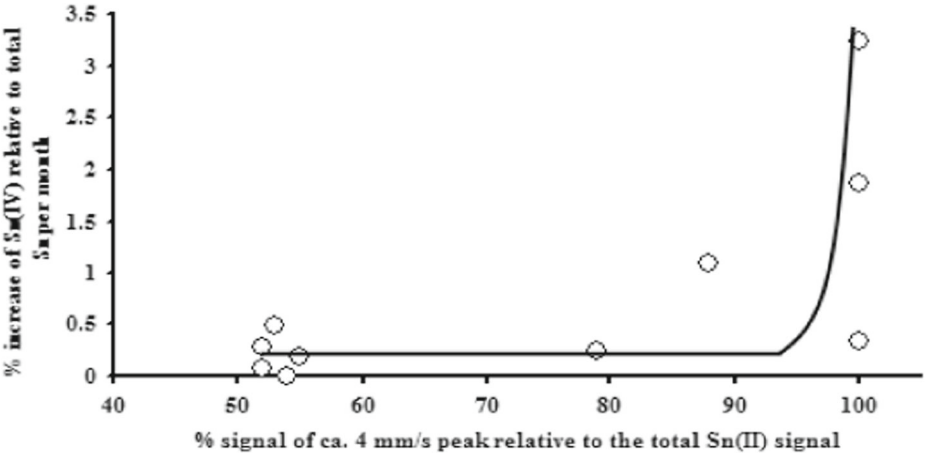

Fig. 22 Percentage increase of the tin(IV) signal relative to the total Sn signal per month, versus the % signal of ca. 4 mm/s peak relative to the total Sn(II) signal. The curve is just a guide for the eye. It was not fitted to any model

faster tin(II) oxidizes (high y regions, B and C), and since the recoil-free fraction is a function of bond strength, the lower the recoil-free fraction the higher the rate of oxidation. The regions rich in Cl (B and C) were found to have a lower recoil-free fraction and a higher oxidation rate. In contrast the region richer in F and Sn favors ... F−Sn−F−Sn−F ... oligomeriztion that provides more stability to tin, hence higher recoil-free fraction and a lower oxidation rate (zone D).

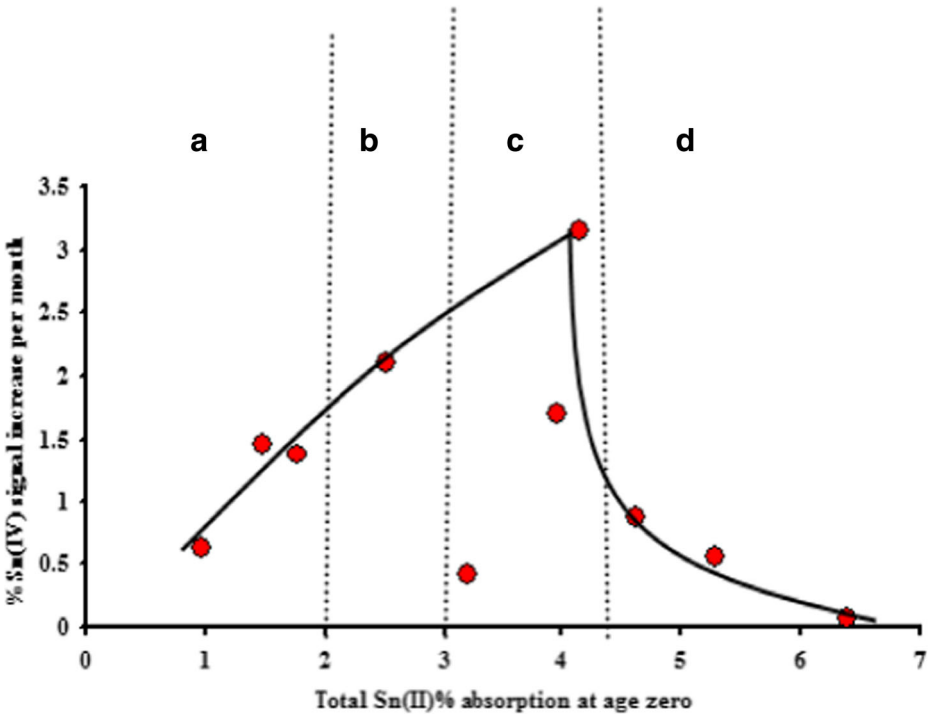

Fig. 23 Percentage tin(IV) signal increase per month versus the total % tin(II) absorption at age zero. Regions A: low *Sn*, medium f_a, B: low *Sn*, high *Cl*, C: high *Sn*, high *Cl*, instability, D: high *Sn*, low *Cl* (i.e. high *F*), high f_a. The curve is just a guide for the eye. It was not fitted to any model

4 Conclusion

The main findings of this study are the following:

a. Divalent tin halides undergo some degree of oxidation to SnO_2 at ambient condition upon storage in air.
b. This SnO_2 is amorphous since it is not detected by X-ray powder diffraction.
c. Due to the very high recoil-free fraction of SnO_2 compared to that of tin(II) halides, Mössbauer spectroscopy is an excellent method for detecting minor amounts of SnO_2. However, the ratio of the intensity of the SnO_2 line over the tin(II) line(s) gives the false impression that the amount of SnO_2 is much higher than it really is.
d. The stoichiometric halides rich in tin passivate well, i.e. after an intial minor oxidation, no further oxidation seems to take place at constant temperature. If the temperature is increased, passivation breaks down and then, after formation of more SnO_2, passivation is restored.
e. It was initially hypothezided that passivation is due to the formation of a surface layer of SnO_2 that protects against further contact between molecular oxygen and tin(II) in the bulk of the particles.
f. Passivation of non-stoichiometric $M_{1-x}Sn_xF_2$ (M= Ca and Pb) for low tin contents works as well as for stoichiometric compounds rich in tin. These non-stoichiometric

solid solutions do not contain enough tin to form a complete passivating layer, therefore the hypothesis of passivation by a layer of SnO_2 is unlikely to be valid.

g. Stoichiometric tin(II) chloride fluorides seem to passivate as well as the fluorides, however passivation in non-stoichiometric doubly-disordered $Ba_{1-x}Sn_xCl_{1+y}F_{1-y}$ is less efficient.

h. In the $Ba_{1-x}Sn_xCl_{1+y}F_{1-y}$ solid solution, ionic Sn^{2+} oxidizes much faster than covalently bonded Sn(II). This is understandable: the weaker the bonds of tin(II) with the surrounding anions, the less energy is required to break it in order to oxidize tin.

i. In the $Ba_{1-x}Sn_xCl_{1+y}F_{1-y}$ solid solution, ionic Sn^{2+} rattles in oversized sites, hence very weak bonding that results in faster oxidation. Covalently bonded tin forms ... F - Sn - F - Sn - F - ... oligomers that have a bond strength similar to that of stoichiometric or non-stoichiometric fluorides, hence a highly efficient passivation.

j. It is probable that other non-stoichiometric tin(II) chloride fluorides would passivate much better than the $Ba_{1-x}Sn_xCl_{1+y}F_{1-y}$ solid solution, that is a special case due to Sn^{2+} ions rattling in oversized site, hence forming no significant amount of bonding.

Acknowledgements This work is dedicated to the memory of Prof. Krzysztof Ruebenbauer, Pedagogical University, Krakow, Poland, who passed away on April 23, 2018. He contributed so much to our understanding of the Mössbauer effect in divalent tin materials.

This work was made possible by the support of Concordia University and the Natural Science and Engineering Research Council of Canada. Grateful thanks are also due to the Procter and Gamble Co. (Mason, Ohio) for supporting our Mössbauer laboratory.

References

1. Dirac, P.A.M.: Principles of Quantum Mechanics. International Series of Monographs on Physics, 4th edn., p. 255. Oxford University Press (1982)
2. Dénès, G.: The "Bent Copper Tube": an inexpensive and convenient reactor for fluorides of metals in suboxidation states. J. Solid State Chem. **77**, 54–59 (1988)
3. Birchall, T., Dénès, G., Ruebenbauer, K., Pannetier, J.: A tin-119 Mössbauer study of the phase transitions in SnF_2. J. Chem. Soc. Dalton, 1831–1836 (1981)
4. Dénès, G., Bell, M.F., Sayer, M.: $BaSnF_4$ – a new fluoride ionic conductor with the α–$PbSnF_4$ structure. Solid State Ion. **13**, 213–219 (1984)
5. Birchall, T., Dénès, G., Ruebenbauer, K., Pannetier, J.: Tin-119 Mössbauer spectroscopic study of a single crystal of α–SnF_2 and partially oriented α–$PbSnF_4$. J. Chem. Soc. Dalton, 2296–2299 (1981)
6. Birchall, T., Dénès, G.: A ^{19}F, ^{119}Sn nuclear magnetic resonance and ^{119}Sn Mössbauer study of the SnF_2 - MF – H2O system. Can. J. Chem. **62**, 591–595 (1984)
7. Lengyel, L., Homonnay, Z., Kuzmann, E., Klencsar, Z., Sipos, P., Bajnoczi, E.G., Palinko, J.: Goldanskii-Karyagin effect in hyperalkaline tin(II) hydroxide. J. Radioanal. Nucl. Chem. **307**, 1195–1201 (2016)
8. Dénès, G., Madamba, M.C.: X-ray diffraction study of phase transformations in superionic $PbSnF_4$ upon milling and subsequent annealing. Mater. Struct. **3**, 227–245 (1996)
9. Dénès, G., Ruebenbauer, K.: GMFP5, an extension of GMFP 58 to five hyperfine sites, unpublished results
10. Ruebenbauer, K., Birchall, T.: A computer programme for the evaluation of Mössbauer data. Hyperf. Interact. **7**, 125–133 (1979)
11. Galy, J., Meunier, G., Andersson, S., Aström, A.: Stéréochimie des éléments comportant des paires non liées: Ge(II), As(III), Se(IV), Br(V), Sn(II), Sb(III), Te(IV), I(V), Xe(VI), Pb(II) et Bi(III) (oxydes, fluorures et oxyfluorures). J. Solid State Chem. **13**, 142–159 (1975)
12. Gillespie, R.J., Nyholm, R.S.: Inorganic stereochemistry. Quart. Rev. Chem. Soc. **11**, 339–380 (1957)
13. Brown, I.D.: Bond valence as an aid to understanding the stereochemistry of O and F complexes of Sn(II), Sb(III), Te(IV), I(V) and Xe(VI). J. Solid State Chem. **11**, 214–233 (1974)
14. Dénès, G., Pannetier, J., Lucas, J., Le Marouille, J.Y.: About SnF_2 stannous fluoride. I. Crystallochemistry of α–SnF_2. J. Sol. State Chem. **30**, 335–343 (1979)
15. Birchall, T., Dénès, G., Ruebenbauer, K., Pannetier, J.: Goldanskii-Karyagin effect in α–SnF_2: a neutron diffraction and Mössbauer absorption study. Hyp. Interact. **30**, 167–183 (1986)

16. Goldanskii, V.I., Marakov, E.F., Stukan, R.A., Samakosova, T.N., Trakhtanov, V.A., Khrapov, V.V.: The Mössbauer effect and its applications. Proc. Acad. Sci. USSR **156**, 474 (1964)
17. Greenwood, N.N., Gibb, T.C.: Mössbauer Spectroscopy, p. 375. Chapman and Hall, London (1971)
18. Dénès, G.: About SnF_2 stannous fluoride. I. Phase transitions. Mater. Res. Bull. **15**, 807–819 (1980)
19. Weast, R.C., Astle, M.J. (eds.): CRC Handbook of Chemistry and Physics, 61st edn. CRC Press, Boca Raton (Unknown Month 1980)
20. Muntasar, A., Le Roux, D., Dénès, G.: Stabilization of the unhybridized Sn^{2+} stannous ion in the BaClF structure and its characterization by ^{119}Sn Mössbauer spectroscopy. J. Radioanal. Nucl. Chem. **190**, 431–437 (1995)
21. Dénès, G., Muntasar, A.: X-ray diffraction and Mössbauer spectroscopic studies of Sn/Ba and Cl/F substitutions in BaClF. Mater. Struct. **3**, 246 (1996)
22. Dénès, G., Muntasar, A.: Bonding in the doubly disordered $Ba_{1-x}Sn_xCl_{1+y}F_{1-y}$ solid solution. Hyp. Interact. **153**, 91–119 (2004)
23. Shannon, R.D., Prewitt, C.T.: Effective ionic radii in oxides and fluorides. Acta Cryst. B **25**, 925–946 (1970)